Characterization of Clay- and Silt-Sized Fractions and Corresponding Humic Acids Along a Terra Rossa Soil Profile

Brunetti, Gennaro; Mezzapesa, Giuseppe Natale; Traversa, Andreina; Bonifacio, Eleonora; Farrag, Karam; Senesi, Nicola; D'Orazio, Valeria. Characterization of Clay- and Silt-Sized Fractions and Corresponding Humic Acids Along a Terra Rossa Soil Profile. CLEAN - SOIL, AIR, WATER. 44 (10) pp: 1375-1384.
DOI: 10.1002/clen.201500857

Characterization of Clay- and Silt-Sized Fractions and Corresponding Humic Acids Along a Terra Rossa Soil Profile

Gennaro Brunetti[1] Giuseppe Natale Mezzapesa[2] Andreina Traversa[1] Eleonora Bonifacio[3] Karam Farrag[4] Nicola Senesi[1] Valeria D'Orazio[1]

[1]Dipartimento di Scienze del Suolo, della Pianta e degli Alimenti, University of Bari, Bari, Italy; [2]CIHEAM, Mediterranean Agronomic Institute of Bari, Valenzano, Bari, Italy; [3]Dipartimento di Scienze Agrarie, Forestali e Alimentari, University of Torino, Grugliasco(TO), Italy; [4]Biology and Environmental Indicators Department of Central Laboratory for Environmental Quality Monitoring (CLEQM), National Water Research Centre (NWRC), Cairo, Egypt

Abstract

This study focuses on the relationship between soil mineralogy and soil organic matter stabilization along a Terra Rossa soil profile in Southern Italy. This soil profile is characterized by three horizons: Namely Ap, 2AB, and 2Bt, where the clay, silt, and sand size fractions were isolated and their mineralogical composition, and the different forms of iron, silicon, and aluminum were determined. Humic acids (HAs) were isolated from clay-size (C-HA) and silt-size (S-HA) fractions, and characterized by chemical and physico-chemical techniques. The clay fraction had the largest amount of amorphous and crystalline oxides, kaolinite, and chlorite. In all fractions, the 2AB horizon differed from the other two horizons showing a very high content of iron and aluminum bound to organic matter (Fe_p and Al_p). Chemical and spectroscopic analyses of humic acids indicated the presence of macromolecules with larger size and polycondensation degree in S-HAs, apparently less susceptible to degradation than simpler hydrophilic compounds occurring in the clay-size HAs. A good correlation was found between Fe_p and Al_p contents and HA organic carbon. These properties are expected to slow down organic matter dynamics in Terra Rossa Mediterranean soils even in the presence of a fast turnover of aggregates.

Keywords: C stabilization; FT-IR and fluorescence spectroscopy; Humic substances; Mineralogical analysis; Particle-size fractions

1 Introduction

Recent studies have focused on C stabilization in soils, in order to reduce CO_2 emissions into the atmosphere and control the greenhouse effect [1, 2], and have showed the existence of strong relationships between soil organic matter (SOM) stabilization and soil Fe and Al oxides, hydroxides, and oxyhydroxides [1, 3]. In particular, findings were: (i) a positive correlation between soil metals and total organic carbon (TOC) concentrations for different soils [4]; (ii) an inverse correlation between soil TOC turnover rates and metal concentrations [5]; (iii) a high sorption capacity of Fe and Al oxyhydroxides [6]; and (iv) the ability of metal complexes to retard microbial/enzymatic mineralization of SOM [7]. Furthermore, both SOM and extractable phases of Fe oxides were positively correlated with aggregate stability in soils [8]. The postulated binding mechanisms were in form of ligand exchange between Fe and Al oxy- or hydroxy groups, and hydr- and carboxyl functions of humic substances [9]. Humic acids (HAs) can be considered the main stable products of humification, in which OC is ftxed in soil in the form of complex macromolecules resistant to chemical and microbial decomposition. The role of the oxides as binding agents that promote the formation of microaggregates, consisting of oxides, SOM, including HAs, and minerals has been widely proved [1]. The formation of microaggregates, of which clay minerals are the principal components, represents the most efficient way to stabilize SOM, depending on several parameters, such as climate and soil properties [2]. In particular, SOM stabilization in soil is significantly influenced by soil texture [10], as the SOM content is generally positively correlated with clay and silt content in soil [11]. In particular, layer silicates can contribute to SOM stabilization through the formation of bridges between exchangeable cations and functional groups of organic compounds [12]. SOM stabilization may be induced either by an increase of the activation energy of organic molecules, due to conformational changes and complexation of reactive groups upon adsorption, or by intercalation within microaggregates and small pores which prevents hydrolytic enzymes to approach the organic substrate [13]. Generally, Terra Rossa soils, that are widespread around the Mediterranean basin, have a clay-rich Bt horizon that may deeply impact organic matter stabilization, and a clayey texture. Kaolinite, hematite, and goethite often dominate the mineralogical composition, and the bottom horizons are typically calcium-rich, thanks to the

calcareous parent material [15, 16]. Due to the high summer temperature of the Mediterranean basin, these soils are particularly prone to organic matter decline [14].

The aim of this work was to investigate the relationships among mineralogical composition, metal oxyhydroxides, and HAs proper- ties in soil clay- and silt-sized fractions isolated from three horizons of a Terra Rossa soil, in order to obtain information about SOM dynamics and C stabilization in the Terra Rossa soils of the Mediterranean regions.

2 Materials and methods

2.1 Study area

The selected soil is a Terra Rossa soil sampled in a field of about 24 ha at the agricultural experimental farm "Agostinielli" of CRA-SCA, located in Rutigliano–Bari, Apulia, Southern Italy (UTM33-WGS84, 671060E-4539796N), and was described according to the sequence of genetic horizons [17]. This soil is on a flat surface currently used as orchards, at an elevation of 125 mL asl. The average annual precipitation in the area is 623 mm, while average temperature is 15.2°C. The soil moisture regime is Xeric. The cultivation consists of scattered olive trees and minimum tillage is regularly practiced to control weeds. Clay translocation was clearly visible in the field through clay skins in the Bt horizon. To avoid small atypical areas, a linear transect sampling method was preliminarily applied in order to verify the soil properties, then a soil profile, approximately 1.5 m deep, was excavated by means of a digger. The profile can be considered representative of the entire farm from which it was sampled. The lithological discontinuity recorded between the Ap and the other soil horizons was related to the amounts of coarse fragments, likely influenced by agricultural practices. The soil was classified as a Mollic Haploxeralf [18], and characterized by three horizons, designated as Ap, 2AB, and 2Bt. Further details on the chemical properties of the selected soil are reported elsewhere [19].

2.2 Separation and analyses of particle-size fractions

To ensure the representativeness of the soil sample the method of quartering was applied. Successively, samples were gently crushed and sieved at 2 mm to obtain the fine earth fraction, which was then size fractionated [20]. Briefly, a soil–water suspension was fractionated by a combination of wet sieving and repeated centrifugation to avoid disruption of microaggregates. Particle size fractions of 200–63 mm (fine sand fraction), 63–2 mm (silt fraction), and <2 mm (clay fraction) were obtained according to Stokes' law. Each size fraction was oven-dried at about 37°C and subsequently weighed in order to determine its weight percentage with respect to the fine earth sample. As no removal of cementing agents was performed, the size classes correspond to sand-, silt-, and clay-sized aggregates, in addition to sand, silt, and clay particles.

The Fe, Al, and Si were extracted from each size fraction of the three horizons using ammonium oxalate [21] (Feo, Alo, Sio) and Na-dithionite-citrate-bicarbonate [22] (Fed, Ald, and Sid). The Fe and Al bound to SOM were isolated by the pyrophosphate method [23] (Fep, Alp). All extracts were centrifuged and filtered for the successive measurements by inductively coupled plasma optical emission spectrometry (ICP-OES) (Thermo Scientiftc, ICAP 6000 Series).

The mineral phase analysis was carried out by X-ray powder diffraction (XRPD) using a PANalytical X'Pert pro MPD, with the Cu-Ka radiation (curve graphite monochromator, 40 kV; 40 mA) from 2 to 70° 2u), at a speed of 0.02° 2u s—1. The oriented mounts were scanned as air-dried, glycerol solvated, and heated. The semi- quantitative mineralogical composition of the different size classes was performed on peak heights, taking into account peak shifts, using both oriented, and randomly oriented mounts, according to the method proposed by Schulz [24] and Shaw [25], and modified by Laviano [26].

Elemental analysis for major elements was obtained by X-ray fluorescence (Siemens D5000 RhKa radiation) on pressed pound disks. The precision for major elements was >5%, while the precision for trace elements was >10%. The loss on ignition (LOI) was determined by heating each sample for 3 h at 900°C.

2.3 Isolation and characterization of humic acids

The HAs were isolated from clay-size (C-HA) and silt-size (S-HA) fraction of each horizon according to Swift's method [27], and each homogenized and freeze–dried sample was characterized for its main chemical, and spectroscopic properties. No HAs have been isolated from the sand-sized fraction because of its inadequate organic matter content.

Carbon, H, N, and S contents were determined using a combustion- gas chromatography technique (Elemental analyzer, Flash 2000, Thermo-Scientiftc). Oxygen content was calculated by difference.

The analyzer was previously calibrated by means of 2,5-bis (5-tert-butyl-benzoxazol-2-yl)-thiophene (BBOT) standard (Thermo- Quest Italia s.p.a.). All HAs were analyzed in triplicate and the obtained data were corrected for moisture and ash contents.

The E4/E6 ratio was calculated on solutions of 3 mg of each HA in 10 mL of 0.05 mL NaHCO3, as the ratio of the absorbance at 465 and 665 nm measured by UV-vis spectrophotometry (PerkinElmer model Lambda 15).

Fourier transform infrared (FT-IR) spectra were acquired in the transmittance mode using a Thermo Nicolet Nexus FT-IR spectrophotometer, equipped with the Nicolet Omnic 6.0 software. Potassium bromide pellets were obtained by pressing homogenized mixtures of 400 mg of IR-grade KBr and 1 mg of each HA, under reduced pressure. Spectra were recorded under N_2 atmosphere in the range of 4000–400 cm^{-1}, with 2 cm^{-1} resolution and 64 scans for each acquisition.

Fluorescence spectra were obtained on aqueous solutions of HAs at a concentration of 10 mg L^{-1} (C concentration comprised between 4 and 5 mg L^{-1}), after overnight equilibration at room temperature and adjustment to pH ~ 8 with 0.05 mL NaOH [28]. Preliminary experiments carried out on samples at different organic C concentration showed no changes due to inner filter effects and/or quenching phenomena. Further, all fluorescence spectra were electronically corrected for instrumental response, and both the sensitivity and stability of the instrument were previously measured using the Raman band signal intensity. Emission and excitation slit widths were set at5 nm, and a scan speed of 1200 nm min—1 was selected for each monochromator. Total luminescence spectra (TL spectra) were recorded in the form of excitation/emission matrix (EEM) spectra (or contour maps) by scanning the wavelength emission over the range 300–600 nm, while the excitation wavelength was increased sequentially by 5 nm steps from 250 to 500 nm. The EEM spectra were generated from TL spectral data by using Surfer 8.01 software (Golden Software, Golden, CO).

2.4 Statistical analysis

Correlations between variables were evaluated using the Pearson's correlation coefficient and differences among size fractions were checked by Duncan's post hoc test after one-way ANOVA with significance level of 0.05.

3 Results and discussion

3.1 Soil chemical and mineralogical properties

The clay-sized aggregate content ranged from 410 to 496 g kg^{-1} (Tab. 1), and increased with depth, due to clay translocation and successive accumulation into the illuvial horizon in the Terra Rossa soil. The silt-sized aggregate content ranged from 401 to 460 g kg^{-1}, with an opposite trend to that of clay-sized. The sand-sized aggregate content was low in the three horizons.

The Fep and Alp were more abundant in the silt fraction ($p < 0.05$),

particularly in the 2AB horizon (Tab. 2). On the contrary, the Sid, Ald, Fed, and Sio, Alo, and Feo were more abundant in the clay fraction, with respect to the silt ones. In particular, values of Sid were similar in the Ap and 2Bt horizons of clay and silt fractions, and lower in the 2AB horizon. The same trend was observed for the Ald, Sio, and Alo. The Fe oxides represented almost the totality of Fe forms in the clay fraction (90–93%, Tab. 2) as indicated by the ratio between Fed and Fet, whereas, the opposite occurred in the sand-sized fraction, where poorly crystalline oxides (Feo) prevailed.

The low proportion of poorly crystalline Fe oxides was in agreement with the results normally obtained in the Mediterranean red soils [16], as well as the large Fed contents in both clay and silt fractions [29]. Aluminum and iron oxyhydroxides are efftcient sorbents for dissolved OM in soils and stream sediments [30, 31], and only 28–35% of sorbed OM can be desorbed from goethiteand hematite [32]. Ferrihydritehas a larger surface area [33], and its point of zero

charge is slightly higher than that of both goethite and hematite (*i.e.*, 8.6 vs. 8.1 and 7.6, respectively) [34]. At the pH of Terra Rossa soils, ferrihydrite should therefore, play a more important role in both OM sorption and aggregation than more crystalline oxides.

Only small differences in mineralogical composition were found among horizons (Fig. 1). The only layer silicates identified by XRPD were kaolinite (Kln) and a degraded form of illite (Ilt). Primary minerals such as quartz (Qz), feldspars (Fsp), and calcite (Cal) were present as well. Greater differences were visible by comparing the clay- and silt- sized fractions (Fig. 2); layer silicates formed almost the totality of the clay fraction (about 95%), and Ilt showed a clear decreasing trend toward the soil surface (Fig. 1). In the sand-sized fraction Qz and Fsp dominated the mineralogical composition. The composition of the silt fraction was intermediate between clay and sand. The Cal was present only in the sand-size fraction, and a strong depletion can be observed in the 2AB horizon. The Kln may be inherited from the parent material or formed in the soil by neogenesis, or transformation reactions [35]. Soil Kln is however, typically of smaller particle size than those of geological deposits [36], hence, has a higher surface area and reactivity. The abundance of the Kln in clays pointed toward its pedogenic origin, as often reported in well-developed soils of Mediterranean environments [37].

The minor presence of the Ilt in the uppermost horizon suggested its degradation through the loss of interlayer K, in agreement with the continuous agricultural use and root abundance [38]. The process has not yet induced the appearance of 1.4 nm layer silicates, nonetheless the visible enlargement of the 1 nm peak depicting the Ilt degradation. The very low contents of the Cal in the 2AB horizon confirmed that agricultural practices have influenced the upper- most horizon, and the larger abundance of this mineral in the sand- sized fraction is in agreement with its lithogenic origin.

The elemental composition of each particle-size fraction of the three horizons is shown in Tab. 3. The SiO_2, Al_2O_3, and Fe_2O_3 were the most represented compounds in the soil, and their concentrations were in agreement with those reported by Bellanca et al. [39] and Palumbo et al. [29], in Terra Rossa soils of Southern Italy.

The SiO_2 and CaO contents were the largest in the sand fraction; the Al_2O_3, Fe_2O_3, and MgO contents were the largest in the clay fraction, whereas, those of the other compounds examined were similar in each fraction of the three horizons. The content of the SiO_2 was the largest and that of the CaO was the lowest in all particle- size fractions of the 2AB horizon, whereas, the contents of the Al_2O_3 and Fe_2O_3 showed no apparent trend in any particle-size fraction of the three horizons. The LOI range was 7.2–14.0% for clay and silt fractions, and was in agreement with the expected values due to the loss of SOM [40], hydration water, and calcite.

The Si/Al molar ratio decreased from 14 to 15 in the sand-sized fraction to 2.6 in clay, in agreement with the decreasing quartz and increasing layer silicate contents, without any specific depth trend, reflecting thus. the poor mineralogical differentiation of soil horizons and the variability among size fractions. The CaO contents were totally explained by the variability of the calcite abundance ($r^2 = 0.979$, $p < 0.01$, $n = 12$).

The results of the correlation matrix are shown in Tab. 4, with significant correlation at $p < 0.01$. A highly significant positive correlation was observed between clay minerals and metal forms; the Kln was very well correlated with all forms of the Al and Fe, except Fep and Alp, which showed a larger correlation with the Ilt contents. Primary minerals (Qz, Fsp, and Cal) showed significant negative correlations with all metal forms.

The combined effect of layer silicates and (hydr)-oxides on organic matter stabilization is highly variable as sorption and desorption change depending on the resulting surface charge. According to Saidy et al. [41], ferrihydrite and goethite can significantly increase the sorption capacity of kaolinitic clays, but goethite has no effect when illite dominates. Although hematite is the most common Fe oxide in Terra Rossa soils, goethite is also reported [15, 16]. Soil classiftcation as a Mollic Haploxeralf (and not as a Rhodoxeralf) suggests the presence of both crystalline oxides; the presence of ferrihydrite can be neglected in clay, due to the low Feo/Fed ratio, but may be more important in the silt fraction. Therefore, depending on the mineralogical composition, the stabilization capacity of organic matter by the mineral phase is expected to be strongly variable as a function of size fractions, and within each fraction between the 2AB and the other soil horizons.

3.2 Chemical and spectroscopic characterization of humic acids

The properties of C- and S-HAs of each horizon are shown in Tab. 5. The extraction yields of C-HAs for all horizons

were much lower than those of S-HAs and in both fractions the maximum HA yield was measured in the 2AB horizon. In general, according to Christensen [42], the C-HAs showed larger N and S contents, and lower O content with respect to those of the corresponding S-HAs. The greater amount of the S observed in the C-HA samples might be due to a preferential adsorption of the SO 2—, organic sulfate esters, and sulfones on surfaces of clay minerals and pedogenic Fe, and Al oxides [43], which are mainly present in the clay fraction of soils. The C-HAs showed narrower C/N ratios for all horizons with respect to those of the corresponding S-HAs. In details, the HAs isolated from the 2AB horizon of both fractions are characterized by the largest C/N ratio values with respect to those measured in the HAs from the other two horizons. On the contrary, the C- and S-HAs from the 2AB horizon showed the lowest H/C ratio, thus, suggesting a larger aromatic character with respect to that of C- and S-HAs from the other two horizons. The (O þ N)/C ratio is an index to evaluate the polar/non-polar balance of the samples. The S-HAs exhibited similar ratio values with respect to those of the C-HAs, with the exception of the S-HA from the 2AB horizon, featured by a lowest value, which means a more hydrophobic character. These results are confirmed by the H/O ratio, generally used as an index of the oxidation degree of the organic matter. In particular, the S-HA sample from the 2AB horizon showed the largest H/O ratio, thus, suggesting relatively low number of oxygen-containing functional groups, relatively low polarity and high hydrophobicity [44].

The E4/E6 ratios of the C-HAs of the three horizons were similar, and larger than those of the S-HAs. According to Chen et al. [45], these results indicate that the C-HAs are characterized, with respect to the S-HAs, by a greater aliphatic character, a smaller molecular weight and larger acidic functional groups content, confirming what previously suggested by elemental analysis. The lowest E4/E6 value reported for the S-HA, especially in the S-HA sample from the 2AB horizon, can be related to greater condensation degree and molecular weights, and to a more aromatic character.

Both the amounts of HA extracted and their chemical properties were related to soil mineralogical composition. Higher yields were obtained from the size fractions with the largest Si/Al ratio ($r = 0.944$, $p < 0.01$, $n = 6$), that can be used as a global indicator of quartz and feldspar abundance with respect to layer silicates. Conversely, a negative correlation was found between HA yields and Fe (hydr)oxides. Both poorly crystalline forms (Feo) and more crystalline oxides (computed as Fed–Feo) were well correlated withHA yields ($r = —0.960$ and $r = —0.929$, respectively, $p < 0.01$, $n = 6$).

The C/N ratio increased with increasing Si/Al ratio ($r = 0.939$, $p < 0.01$, $n = 6$) and with decreasing amount of Fe (hydr)oxides either crystalline ($r = —0.31$, $p < 0.05$, $n = 6$), or poorly crystalline ($r = —0.851$, $p < 0.05$, $n = 6$) and kaolinite ($r = —0.812$, $p < 0.05$, $n = 6$). Similar correlations were found for the E4/E6 ratio, with Pearson's correlation coefftcients of: —0.951, —0.969, and —0.910 for the Si/Al ratio, quartz, and feldspars, respectively, and 0.984, 0.943, and 0.970 for crystalline and poorly crystalline Fe forms, and kaolinite. No signiftcant correlations were instead observed with the degree of aliphaticity or the indicator of polarity of the HAs. All these correlations suggest that the characteristics of the HAs released from clay- and silt-sized fractions differ depending on whether primary or pedogenic minerals dominate the fraction.

The FT-IR spectra of the HAs isolated from the clay- and silt-size fractions of the different horizons (Fig. 3) are typical of soil HAs [46, 47], and characterized by the presence of several common absorption bands with some differences in their relative intensity as a function of their source, both as size fraction and as horizon.

In detail, FT-IR spectra of the C-HAs featured a more intense absorption at 2924 and 2853 cm^{-1} (asymmetric and symmetric C—H stretching of CH_2 groups, respectively), and at 1240 cm^{-1} (C–O stretching and OH bending of COOH groups, and phenols) in the C-HA from the 2AB horizon, and a slight increase of the band intensity at 1715 cm^{-1} (C=O stretching of various carbonyl groups including COOH) when passing from the Ap to the 2AB horizon. Differently, FT-IR spectra of the S-HAs were characterized along the profile by a decrease of the absorption bands at 2924 and 2853 cm^{-1}, and by the disappearance of absorption bands at 1117 and 1026 cm^{-1}. Infrared spectroscopy indicates that the C-HAs were characterized, in comparison with the S-HAs, by a greater number of carboxylic groups, although they showed lower oxygen content. This means that more oxidized organic molecules occurred in the C-HAs with respect to the S-HAs, and according to Zech et al. [48], the greater oxidation degree can be directly related to the presence of more humified molecules. On the contrary, the larger oxygen contents measured in the S-HAs, with the exception of the HA from the 2AB horizon, could be reasonably ascribed to a larger

amount of hydrophobic O-containing molecular structures.

The fluorescence EEM matrices of the HAs isolated from the clay and silt fractions of the different horizons are shown in Fig. 4. All the HAs were characterized by the presence of a main common fluorophore, identifted by the excitation/emission wavelength pair (EEWP) of 440–445ex/510–514em, in the C-HAs, and 445–450ex/518–524em in the S-HAs. In general, these wavelengths indicate the presence of very complex structures, such as quinones and phenols with an extended polycondensation degree [28]. In particular, the EEM spectra of the S-HAs showed a red-shift of the excitation and, especially, of emission wavelengths of this fluorophore with respect to those of the corresponding C-HAs. Furthermore, the fluorescence intensity (FI) values of the C-HAs were always much larger than those of the corresponding S-HAs. According to D'Orazio et al. [49], smaller FI values and longer wavelengths can be attributed to large-molecular weight components possessing linearly-condensed aromatic ring systems bearing electron-withdrawing substituents, such as carbonyl and carboxyl groups, and/or to other unsaturated bond systems, such as Schiff-base structures, capable of a great degree of conjugation. Conversely, larger FI values and shorter wavelengths can be ascribed to simpler structural components of low MW and bearing electron-donating substituents, such as hydr-, methoxyl, and amino groups, small degree of aromatic polycondensation, and small level of conjugated chromophores [50]. The obtained results clearly indicate a different structural complexity between the examined HAs as a function of the particle size fraction. The red-shift in the EEWPs of the S-HA suggests a greater molecular complexity and presence of more extended p-electron systems. These results appeared completely in agreement with those found by Manjaiah et al. [51] and Christensen [42], who found, respectively: (i) a direct correlation between aromatic C content and increasing particle size; and (ii) the great presence of alkyl-C deriving from microbial products in the clay-organic matter complexes, and of aromatic residues (i.e., lignin moieties) originated from plant residues in the silt-organic matter complexes.

Relatively to the examined horizons, the EEM spectra showed an increasing FI values of the C-HAs downward the profile, thus, suggesting the presence of less complex molecular structures with increasing depth. Differently, a particular pattern is shown by the S-HA from the 2AB horizon that showed the lowest FI value with respect to those of the other two horizons, thus, confirming the presence of more complex molecules with a larger polycondensation degree in this horizon. These results might be related to the larger content of Alp and Fep coordinated by HAs in the silt-size fraction as compared to that of the corresponding clay-size fraction. As reported in a previous study [52], molecules with high molecular weight can interact by a large number of ligands with the mineral surface yielding very stable bonds. Consistently with Eckmeier et al. [53], Fep and Alp contents correlated well to the organic C content of the HAs isolated from clay and silt fractions (Fep, $r = 0.869$, $n = 4$, p Ç 0.05; Alp, $r = 0.905$, $n = 4$, $p < 0.05$).

Organic molecules can bind to minerals through several mechanisms, depending on the characteristics of both organic and mineral phases involved in the association. According to the zonal model developed by Kleber et al. [54], polar groups of amphiphiles strongly interact with the hydroxyls of mineral surfaces (silicates and hydroxides) and create a contact zone; the hydrophobic portions of these molecules can in turn associate with other hydrophobic moieties that are, therefore, less strongly retained than those of the contact zone. An outer region further develops due to cation bridging and hydrogen bonding, where organic compounds are only loosely retained. Clay-sized aggregates of this Terra Rossa soil are expected to be richer in stabilized C than the larger sized fractions, due to the abundance of (hydr)oxides, both crystalline and poorly crystalline, and the greater presence of layer silicates that may provide additional sites for sorption through cation bridges. However, the amounts of the HAs extracted from clay-size were systematically lower and of lower molecular complexity, than those obtained from silt-size fractions. At the clay level, the interaction should consist in the formation of clay- polyvalent cations-organic matter units, according to the C-P-OM model of aggregation developed by Edwards et al. [55], and should involve both the contact and the outer zones. Due to the high pH (7.7–7.9, Traversa et al. [19]), and the presence of calcite, Ca is the dominant polyvalent basic cation in this soil, but binding of organic matter through Ca bridges should have allowed the release of more humic substances upon the HCl wash in the NaOH extraction. In Terra Rossa soils an extensive covering of Fe oxides on layer silicates is expected, thus, inducing a greater stabilization of organic matter by interaction with minerals surfaces through ligand exchange. Dispersible complexes between organic matter and Fe or Al, and poorly crystalline oxides are present in very low amounts with respect to dominating crystalline forms,

but the C-HA characteristics appear to be consistent with poorly complexed aliphatic com- pounds. Silt-sized aggregates, in turn, form through the union of C-P-OM units and primary particles. The mineralogical composition of the silt-sized fraction evidenced the abundance of quartz and feldspars that, due to the lack of layer charge, are poorly effective in chemical stabilization of both carbon and aggregates. As a result, a greater yield of the HAs could be obtained from silt fractions. Furthermore, the S-HAs are characterized, with respect to the C-HAs, by a larger degree of polycondensation and a greater hydrophilicity, thus, conftrming the hypothesis that more complex molecules that strongly interact with charged minerals can be released due to the presence of non-charged minerals as weakness points in silt sized aggregates. The same trend is obtained if the sequence of soil horizon is analyzed. The 2AB horizon differs from the other ones both in terms of quantity and quality of extracted HAs, in addition to its mineralogical composition featured by greater amounts of calcite. In this horizon, therefore, in addition to quartz and feldspars, the effective stabilizing capacity of oxides is further reduced by the occurrence of calcite that does not seem to act in stabilizing organic matter.

4 Concluding remarks

The present study shows that, the differences between the particle- size-fractions and between the horizons of a Terra Rossa proftle are related to their speciftc mineralogical composition, and their content of Al and Fe oxides. The 2AB horizon appears unique in its characteristic, while the other two horizons result similar.

The hierarchical model of aggregation involves larger C contents with increasing size classes and a sort of hierarchy in OM complexity was also visible from our results, with important implication on OM dynamics. The chemical and spectroscopic characterization of the HAs indicates that humic molecules sorbs to mineral surfaces in a discrete zonal sequence, as a function of their amphiphilicity. At the clay-sized level metal oxides, also in the form of coatings on silicate surfaces, deeply stabilize organic compounds, and only few HAs of low molecular complexity were extracted. With increasing size classes, the larger amount of hydrophobic O-containing molecular structures promotes weaker organo–mineral associations than that in the clay- size aggregates, as proved by the complexity of the released HAs as well as the corresponding extracted amounts. In general, the molecular structures observed in the silt-size HAs are intrinsically less prone to degradation than simpler hydrophilic compounds, thus, even a fast turnover of aggregates may not immediately involve similarly fast OM dynamics in Terra Rossa Mediterranean soils.

Acknowledgments

This work was partially supported by the Ministry of University and Research, Research Project of National Relevance—2008. The authors wish to thank Prof. Rocco Laviano and Dr. Mauro Pallara, of the Dipartimento di Scienze della Terra e Geoambientali, University of Bari, for their valuable suggestions. The Apulia Region Project RELA- VALBIOR is acknowledged for the use of Elemental analyzer, Flash 2000, Thermo-Scientiftc and PerkinElmer model Lambda 15 UV-vis spectrophotometer.

The authors have declared no conflict of interest.

References

[1] J. Six, R. T. Conant, E. A. Paul, K. Paustian, Stabilization Mechanisms of Soil Organic Matter: Implications for C-saturation of Soils, Plant Soil 2002, 241, 155–176.

[2] J. Six, H. Bossuyt, S. Degryze, K. Denef, A History of Research on the Link Between (Micro)Aggregates, Soil Biota, and Soil Organic Matter Dynamics, Soil Till. Res. 2004, 79, 7–31.

[3] K. Denef, J. Six, R. Merckx, K. Paustian, Short-Term Effects of Biological and Physical Forces on Aggregate Formation in Soils With Different Clay Mineralogy, Plant Soil 2002, 246, 185–200.

[4] K. Kaiser, G. Guggenberger, The Role of Dom Sorption to Mineral Surfaces in the Preservation of Organic Matter in Soils, Org. Geochem. 2000, 31, 711–725.

[5] M. S. Torn, S. E. Trumbore, O. A. Chadwick, P. M. Vitousek,
D. M. Hendricks, Mineral Control of Soil Organic Carbon Storage and Turnover, Nature 1997, 389, 170–173.

[6] E. Tipping, The Adsorption of Aquatic Humic Substances by Iron Oxides, Geochim. Cosmochim. Acta 1981, 45, 191–199.

[7] J. P. Boudot, B. A. Bel Hadj, R. Steiman, F. Seigle-Murandi, Biodegradation of Synthetic Organo-Metallic Complexes of Iron and Aluminum With Selected Metal to Carbon Ratios, Soil Biol. Biochem. 1989, 21, 961–966.
[8] S. W. Duiker, F. E. Rhoton, J. Torrent, N. E. Smeck, R. Lal, Iron (Hydr) Oxide Crystallinity Effects on Soil Aggregation, Soil Sci. Soc. Am. J. 2003, 67, 606–611.
[9] M. Schnitzer, Special Publication No. 17, in Interactions of Soil Minerals With Natural Organics and Microbes, (Eds.: P. M. Huang, M. Schnitzer), Soil Science Society of America, Madison, WI 1986, pp. 77–101.
[10] W. J. Parton, D. S. Schimel, C. V. Cole, D. S. Ojima, Analysis of Factors Controlling Soil Organic Matter Levels in Great Plains Grasslands, Soil Sci. Soc. Am. J. 1987, 51, 1173–1179.
[11] M. V. Cheshire, C. Dumat, A. R. Fraser, S. Hillier, S. Staunton, The Interaction Between Soil Organic Matter and Soil Clay Minerals by Selective Removal and Controlled Addition of Organic Matter, Eur. J. Soil Sci. 2000, 51, 497–509.
[12] R. Mikutta, C. Mikutta, K. Kalbitz, T. Scheel, K. Kaiser, R. Jahn, Biodegradation of Forest Floor Organic Matter Bound to Minerals via Different Binding Mechanisms, Geochim. Cosmochim. Acta 2007, 71, 2569–2590.
[13] G. Guggenberger, K. M. Haider, in Interactions Between Soil Particles and Microorganisms. (Eds.: P. M. Huang, J. M. Bollag, N. Senesi), John Wiley & Sons, Chichester 2002, pp. 267–322.
[14] P. Zdruli, R. J. A. Jones, L. Montanarella, Organic Matter in the Soils of Southern Europe, European Soil Bureau Technical Report, EUR 21083 EN, Offtce for Offtcial Publications of the European Communities, Luxembourg 2004.
[15] G. Durn, F. Ottner, D. Slovenec, Mineralogical and Geochemical Indicators of the Polygenetic Nature of Terra Rossa in Istria, Croatia, Geoderma 1999, 91 (1–2), 125–150.
[16] N. A. Jordanova, D. Jordanova, Q. Liu, P. Hu, P. Petrov, E. Petrovsk´y, Soil Formation and Mineralogy of a Rhodic Luvisol—Insights From Magnetic and Geochemical Studies, Global Planet. Change 2013, 110, 397–413.
[17] P. J. Schoeneberger, D. A. Wysocki, E. C. Benham, W. D. Broderson, Field Book for Describing and Sampling Soils. Version 2.0 USDA-NRCS, US Government Printing Offtce, Washington, DC 2002.
[18] Soil Survey Staff. Keys to Soil Taxonomy, 10th ed., USDA -NRCS, Washington, DC 2006.
[19] A. Traversa, V. D'Orazio, G. N. Mezzapesa, E. Bonifacio, K. Farrag, N. Senesi, G. Brunetti, Effects of Soil Texture on the Stabilization of Soil Organic Carbon Along Two Alftsol Proftles: Investigations of Humic Acids and Dissolved Organic Matter, Chemosphere 2014, 111, 184–194.
[20] L. Jocteur Monrozier, J. N. Ladd, A. W. Fitzpatrick, R. C. Foster, M. Raupach, Components and Microbial Biomass Content of Size Fractions in Soils of Contrasting Aggregation, Geoderma 1991, 49, 37–62.
[21] U. Schwertmann, Differenzierung der Eisenoxide des Bodens durch Extraktion mit saurer Ammoniumoxalat-Lo€sung, Z. Pflanzenernahr. Bodenkd. 1964, 105, 194–202.
[22] O. P. Mehra, M. L. Jackson, Iron Oxide Removal From Soils and Clays by Dithionite-Citrate Systems Buffered With Sodium Bicarbonate, Clay Clay Miner. 1960, 7, 317–327.
[23] J. E. McKeague, J. E. Brydon, N. M. Miles, Differentiation of Forms of Extractable Iron and Aluminium in Soil, Soil Sci. Soc. Am. J. 1971, 35, 33–38.
[24] L. G. Schulz, Quantitative Interpretation of Mineralogical Composition From X-Ray and Chemical Data for the Pierre Shale. U.S. Geological Survey Professional Paper 391-C U.S. Geological Survey, Reston, VA 1964. pp. 1–31.
[25] D. B. Shaw, R. G. Stevenson, C. E. Weaver, W. F. Bradley, Procedures in Sedimentary Petrology. (Ed.: R. E. Carver), Wiley, New York 1971,pp. 554–557.
[26] R. Laviano, L. Dell'Anna, in Procedure di Analisi di Materiali Argillosi. Collana di studi ambientali Ente Nazionale Energie Alternative (ENEA), Santa Teresa, Lerici (Sp) 1987. pp. 215–234.
[27] R. S. Swift, et al. in SSSA Book Series No. 5. (Eds.: D. L. Sparks, A. L. Page, P. A. Helmke, R. H. Loeppert, P. N. Soltanpour, M. A. Tabatabai, C. T. Johnston), ASA and SSSA, Madison, WI 1996, pp. 1011–1069.
[28] N. Senesi, T. M. Miano, M. R. Provenzano, G. Brunetti, Characteriza-tion, Differentiation, and Classiftcation of Humic Substances by Fluorescence Spectroscopy, Soil Sci. 1991, 152, 259–271.
[29] B. Palumbo, M. Angelone, A. Bellanca, C. Dazzi, S. Hauser, R. Neri, J. Wilson, Influence of Inheritance and Pedogenesis on the Metal Distribution in Soils of Sicily, Italy, Geoderma 2000, 95, 247–266.
[30] K. Kaiser, W. Zech, Dissolved Organic Matter Sorption by Mineral Constituents of Subsoil Clay Fractions, J. Plant Nutr. Soil Sci. 2000, 163, 531–535.
[31] R. Kiem, I. Ko€gel-Knabner, Organic Carbon in Relation to Mineral Surface Area and Iron Oxides in Fractions <6mm, Org. Geochem. 2002, 33, 1699–1713.
[32] M. B. Benke, A. R. Mermut, H. Shariatmadari, Retention of Dissolved Organic Carbon From Vinasse by a Tropical Soil, Kaolinite, and Fe-Oxides, Geoderma 1999, 91, 47–63.
[33] D. L. Sparks, Environmental Soil Chemistry, 2nd ed., Elsevier Science, Newark, DE, USA 2003. pp. 43–72.
[34] K. Kaiser, G. Guggenberger, Mineral Surfaces and Soil Organic Matter, Eur. J. Soil Sci. 2003, 54, 219–236.

[35] J. B. Dixon, Book Series No. 1, in Minerals in Soil Environments, (Eds.: J. B. Dixon, S. B. Weed), Soil Science Society America, Madison, WI, USA 1989, pp. 467–526.
[36] M. J. Wilson, The Origin of Clay Minerals in Soils: Past, Present, and Future Perspectives, Clay Miner. 1999, 34, 7–25.
[37] A. Sandler, Clay Distribution over the Landscape of Israel: From the Hyper-Arid to the Mediterranean Climate Regimes, Catena 2013, 110, 119–132.
[38] M. M. Mortland, K. Lawton, G. Uehara, Alteration of Biotite to Vermiculite by Plant Growth, Soil Sci. 1956, 82, 477–481.
[39] A. Bellanca, S. Hauser, R. Neri, B. Palumbo, Mineralogy and Geochemistry of Terra Rossa Soils, Western Sicily: Insights Into Heavy Metal Fractionating and Mobility, Sci. Total Environ 1996, 193, 57–67.
[40] J. I. Santisteban, R. Mediavilla, E. Lopez-Pamo, C. J. Dabrio, M. B. R. Zapata, M. J. G. Garcıa, S. Castano, et al. Loss on Ignition: A Qualitative or Quantitative Method for Organic Matter and Carbonate Mineral Content in Sediments? J. Paleolimnol. 2004, 32, 287–299.
[41] A. R. Saidy, R. J. Smernik, J. A. Baldock, K. Kaiser, J. Sanderman, The Sorption of Organic Carbon Onto Differing Clay Minerals in the Presence and Absence of Hydrous Iron Oxide, Geoderma 2013, 209–210, 15–21.
[42] B. T. Christensen, Physical Fractionation of Soil and Structural and Functional Complexity in Organic Matter Turnover, Eur. J. Soil Sci. 2001, 52, 345–353.
[43] J. Prietzel, J. Thieme, M. Salom`e, H. Knicker, Sulfur K-Edge Xanes Spectroscopy Reveals Differences in Sulfur Speciation of Bulk Soils, Humic Acid, Fulvic Acid, and Particle Size Separates, Soil Biol. Biochem. 2007, 39, 877–890.
[44] F. De Paolis, J. Kukkonen, Binding of Organic Pollutants to Humic and Fulvic Acids: Influence of Ph and the Structure of Humic Material, Chemosphere 1997, 34, 1693–1704.
[45] Y. Chen, N. Senesi, M. Schnitzer, Information Provided on Humic Substances by E4/E6 Ratios, Soil Sci. Soc. Am. J. 1977, 41, 352–358.
[46] F. J. Stevenson, Genesis, Composition, Reactions, 2nd ed., Wiley, New York 1994.
[47] A. Traversa, D. Said-Pullicino, V. D'Orazio, G. Gigliotti, N. Senesi, Properties of Humic Acids in Forest Soils: Influence of Different Plant Covering, Eur. J. Forest Res 2011, 130 (6), 1045–1054.
[48] W. Zech, I. Ko€gel-Knabner, Flux Control in Biological Systems. (Ed.: E. D. Schulze), Academic Press, San Diego 1994, pp. 303–334.
[49] V. D'Orazio, A. Traversa, N. Senesi, Forest Soil Organic Carbon Dynamics as Affected by Plant Species and Their Corresponding Litters: A Fluorescence Spectroscopy Approach, Plant Soil 2014, 374, 473–484.
[50] N. Senesi, V. D'Orazio, Encyclopedia of Soils in the Environment. (Ed.: D. Hillel), Elsevier Science, London 2005, pp. 35–52.
[51] K. M. Manjaiah, S. Kumar, M. S. Sachdev, P. Sachdev, S. C. Datta, Study of Clay-Organic Complexes, Curr. Sci. India 2010, 98, 915–921.
[52] B. Gu, J. Schmitt, Z. Chen, L. Liang, J. F. McCarthy, Adsorption and Desorption of Natural Organic Matter on Iron Oxide: Mechanisms and Models, Environ. Sci. Technol. 1994, 28, 38–46.
[53] E. Eckmeier, M. Egli, M. W. I. Schmidt, N. Schlumpf, M. No€tzli, N. Minikus-Stary, F. Hagedorn, Preservation of Fire-Derived Carbon Compounds and Sorptive Stabilization Promote the Accumulation of Organic Matter in Black Soils of the Southern Alps, Geoderma 2010, 159, 147–155.
[54] M. Kleber, P. Sollins, R. Sutton, A Conceptual Model of Organo-Mineral Interactions in Soils: Self-Assembly of Organic Molecular Fragments Into Zonal Structures on Mineral Surfaces, Biogeochemistry 2007, 85, 9–24.
[55] Edwards, J. M. Bremner, Microaggregates in Soils, J. Soil Sci. 1967, 18, 64–73.

Table 1. Size-fraction distribution of three horizons of the soil profile

Horizon	<2 *m*m	2–63 *m*m (slit) g kg^{-1}	>63 *m*m
Ap	410	460	120
2AB	463	434	102
2Bt	496	401	104

Table 2. Element concentrations (mean ± SD, *n* = 3) obtained through chemical extraction

	Si_d (g kg^{-1})	Al_d (g kg^{-1})	Fe_d (g kg^{-1})	Si_o (g kg^{-1})	Al_o (g kg^{-1})	Fe_o (g kg^{-1})	Al_p (mg kg^{-1})	Fe_p (mg kg^{-1})	Fe_d/Fe_{tot}	Fe_o/Fe_d
Clay										
Ap	4.00 ± 0.03	4.79 ± 0.10	60.12 ± 0.77	2.37 ± 0.05	4.48 ± 0.10	3.84 ± 0.13	6.3 ± 0.3	2.3 ± 0.23	0.90	0.06
2AB	3.31 ± 0.14	3.96 ± 0.02	63.11 ± 1.87	1.72 ± 0.08	3.97 ± 0.20	4.02 ± 0.22	17.5 ± 1.4	6.7 ± 0.54	0.93	0.06
2Bt	4.08 ± 0.05	4.63 ± 0.03	61.46 ± 0.78	2.17 ± 0.06	4.13 ± 0.07	3.72 ± 0.15	6.5 ± 0.5	1.7 ± 0.22	0.92	0.06
Silt										
Ap	0.15 ± 0.00	2.03 ± 0.06	24.08 ± 0.94	1.08 ± 0.09	2.53 ± 0.21	2.86 ± 0.23	8.2 ± 0.9	3.2 ± 0.31	0.47	0.12
2AB	0.08 ± 0.00	1.22 ± 0.05	18.65 ± 0.43	0.61 ± 0.01	1.72 ± 0.02	2.45 ± 0.04	28.5 ± 2.4	11.1 ± 1.1	0.42	0.13
2Bt	0.17 ± 0.01	2.03 ± 0.02	23.97 ± 0.16	1.23 ± 0.16	2.49 ± 0.06	3.04 ± 0.06	11.2 ± 3.0	3.9 ± 1.44	0.48	0.13
Sand										
Ap	0.30 ± 0.08	0.30 ± 0.07	0.55 ± 0.13	0.16 ± 0.01	0.24 ± 0.01	0.71 ± 0.05	0.1 ± 0.05	0.4 ± 0.26	0.04	---
2AB	0.33 ± 0.02	0.33 ± 0.03	0.60 ± 0.07	0.18 ± 0.00	0.26 ± 0.02	0.90 ± 0.06	0.9 ± 0.09	0.2 ± 0.05	0.04	---
2Bt	0.33 ± 0.06	0.32 ± 0.05	0.62 ± 0.16	0.17 ± 0.02	0.22 ± 0.01	0.76 ± 0.06	6.7 ± 0.2	0.6 ± 0.42	0.04	---

Si_d, Al_d, Fe_d: Obtained with the Na-dithionite-citrate-bicarbonate extraction. Al_o, Fe_o: Obtained with the ammonium oxalate extraction.
Al_p, Fe_p: Obtained with the ammonium pyrophosphate extraction. Fe_{tot}: Total Fe.

Table 3. Mineralogical composition of each fraction and soil fine earth of the three horizons examined

	%											
Terra Rossa soil	SiO_2	Al_2O_3	Fe_2O_3	CaO	K_2O	MgO	Na_2O	P_2O_5	MnO	TiO_2	LOI‡	Si/Al
<2 *m*m Ap												
	44.2	24.6	9.5	2.0	2.6	1.5	0.1	1.0	0.4	0.1	14.0	2.6
2AB	45.2	25.1	9.7	1.2	2.6	1.5	0.2	1.0	0.3	0.1	13.1	2.7
2Bt	44.4	25.2	9.6	1.6	2.4	1.5	0.1	0.9	0.3	0.1	13.7	2.6
2–63 *m*m												
Ap	53.2	20.9	7.4	2.1	2.8	1.3	0.2	1.1	0.6	0.1	10.4	3.7
2AB	60.5	18.2	6.3	1.0	3.1	1.2	0.2	1.2	1.0	0.1	7.2	4.9
2Bt	54.4	20.7	7.2	1.9	2.7	1.3	0.2	1.1	0.6	0.1	9.8	3.9
>63 *m*m												
Ap	62.6	6.2	2.1	15.2	2.3	0.6	0.2	0.3	0.5	0.0	9.9	14.8
2AB	80.9	8.4	2.3	1.6	3.4	0.5	0.2	0.3	0.8	0.1	1.3	14.2
2Bt	64.8	6.7	2.4	15.3	2.5	0.4	0.3	0.3	0.5	0.0	6.7	14.2

‡ LOI: Loss on ignition.

Table 4. Correlation matrix between elemental composition and metal extraction

	Si_d	Al_d	Fe_d	Si_o	Al_o	Fe_o	Al_p	Fe_p	Fe_{Tot}	Ilt	Kln	Qz	Fsp	Cal
Si_d	1.00													
Al_d	0.92	1.00												
Fe_d	0.91	0.99	1.00											
Si_o	0.87	0.99	0.96	1.00										
Al_o	0.83	0.98	0.97	0.98	1.00									
Fe_o	0.72	0.92	0.94	0.93	0.98	1.00								
Al_p	−0.04	0.13	0.24	0.11	0.25	0.39	1.00							
Fe_p	−0.03	0.16	0.26	0.14	0.29	0.43	0.98	1.00						
Fe_{Tot}	0.73	0.93	0.95	0.94	0.98	0.99	0.39	0.42	1.00					
Ilt	0.54	0.79	0.81	0.80	0.87	0.93	0.61	0.65	0.94	1.00				
Kln	0.95	0.98	0.99	0.94	0.94	0.88	0.16	0.18	0.89	0.73	1.00			
Qz	−0.74	−0.92	−0.94	−0.92	−0.96	−0.97	−0.45	−0.47	−0.98	−0.95	−0.88	1.00		
Fsp	−0.86	−0.92	−0.94	−0.89	−0.91	−0.87	−0.37	−0.39	−0.89	−0.83	−0.93	0.95	1.00	
Cal	−0.38	−0.60	−0.61	−0.62	−0.68	−0.74	−0.40	−0.46	−0.73	−0.75	−0.54	0.63	0.45	1.00

Correlation signiftcant of the 0.01 level.

Table 5. Elemental composition[m] (moisture and ash free), atomic ratios and E_4/E_6 ratios of clay and silt HA-fractions isolated from the different horizons examined

	%										g
	–kg^{-1}										
Terra Rossa soil	N	C	H	S	O	C/N	H/C	(O þ N)/C	H/O	E_4/E_6	HA yield
<2 *m*m Ap											
	5.4±0.2	58.9 ± 0.7	4.9 ± 0.3	0.24 ± 0.1	30.7	12.8	1.0	0.47	2.5	6.57	0.7
2AB	4.9±0.0	60.6 ± 0.1	4.3 ± 0.1	0.22 ± 0.1	30.2	14.6	0.8	0.44	2.2	6.62	1.4
2B±	5.0±0.1	59.7 ± 0.3	4.4 ± 0.1	0.23 ± 0.1	30.7	14.0	0.9	0.46	2.3	7.02	0.9
2–63 *m*m											
Ap	4.4±0.1	57.7 ± 0.7	4.9 ± 0.1	0.10 ± 0.3	33.0	15.4	1.0	0.49	2.4	5.15	6.0
2AB	3.6±0.1	62.9 ± 2.1	4.6 ± 0.1	0.06 ± 0.5	29.0	20.6	0.9	0.39	2.6	4.81	7.2
2B±	3.8±0.0	59.0 ± 0.6	4.7 ± 0.0	0.08 ± 0.4	32.5	18.2	1.0	0.47	2.3	5.17	3.7

[m]Average values (three repetitions)and SD on mean value.

Figure 1. Mineralogical composition of each fraction of the three horizons examined.

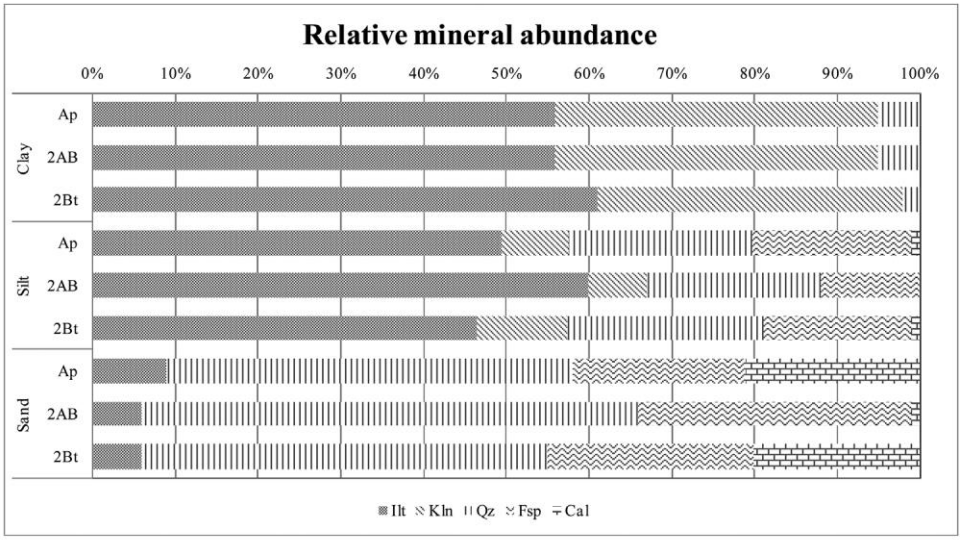

Ilt: Illite
Kln: Kaolinite
Qz: Quartz
Fsp: Feldspar
Cal: Calcite

Figure 2. XRD patterns of air-dry oriented samples of the clay-sized (a) and silt-sized (b) fractions. *d* values are in Å; only the most intense peaks of each mineral are labeled.

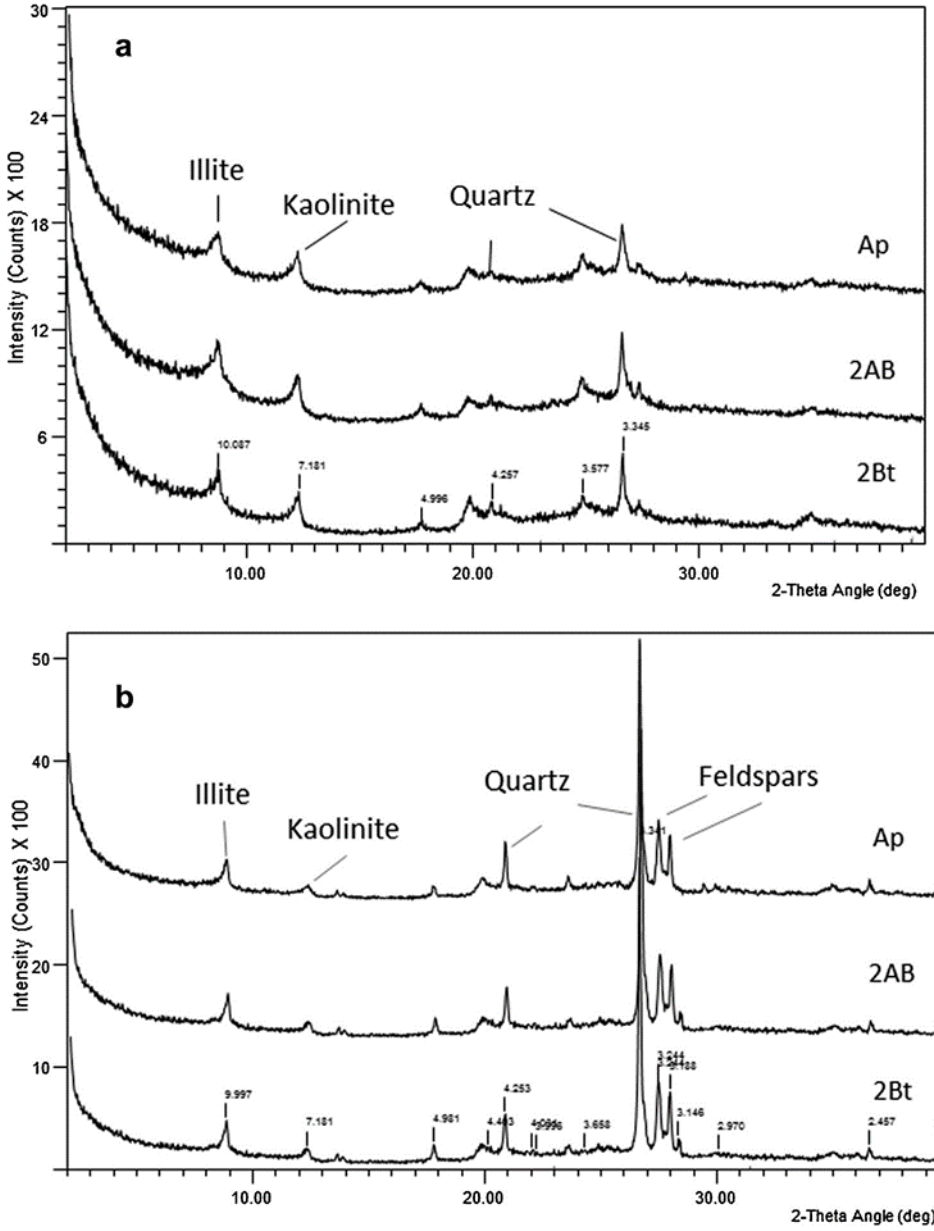

Figure 3. FT-IR spectra of HAs isolated from clay (a) and silt (b) fractions of the three horizons examined.

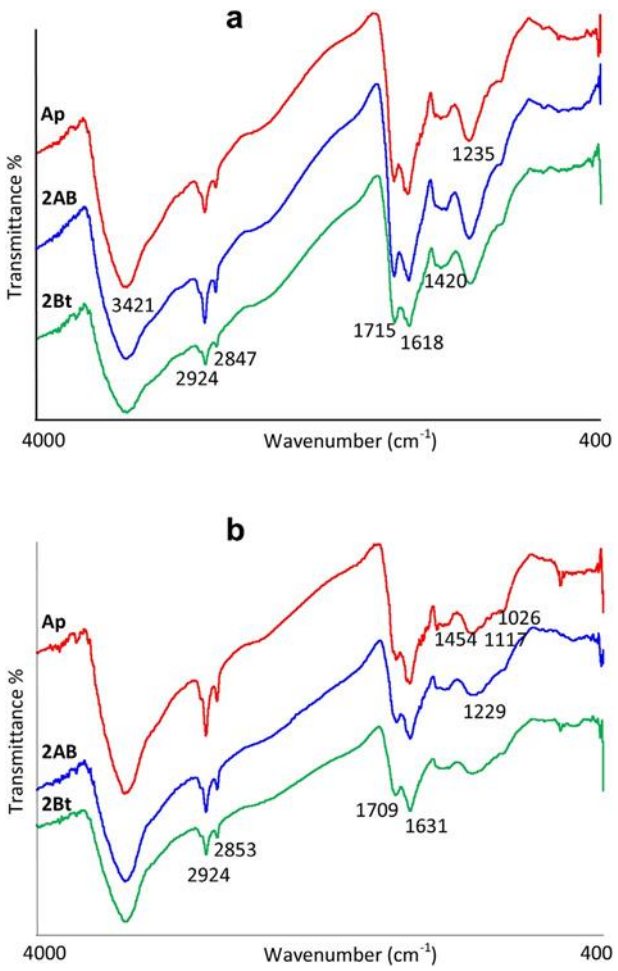

Figure 4. Fluorescence EEMs of HAs isolated from clay (a) and silt (b) fractions of the three horizons examined